Journal of Alloys and Compounds 774 (2019) 515–521

Contents lists available at ScienceDirect

Journal of Alloys and Compounds

journal homepage: http://www.elsevier.com/locate/jalcom

Evolution of structure, magnetism and ferroelectricity in the (1-x)$BiFeO_3$-$xBa_{0.5}Sr_{0.5}MnO_3$($0 \le x \le 1$) solid solutions

J. Wu [a, b], J.F. Zhou [a, b], J.Y. Song [a, b], D. Wang [a, b], X.B. Zhu [a], Y.P. Sun [c, a, d], L.H. Yin [a, *], W.H. Song [a, **]

[a] Key Laboratory of Materials Physics, Institute of Solid State Physics, Chinese Academy of Sciences, Hefei 230031, People's Republic of China
[b] University of Science and Technology of China, Hefei 230026, People's Republic of China
[c] High Magnetic Field Laboratory, Chinese Academy of Sciences, Hefei 230031, People's Republic of China
[d] Collaborative Innovation Center of Advanced Microstructures, Nanjing University, Nanjing 210093, People's Republic of China

ARTICLE INFO

Article history:
Received 29 June 2018
Received in revised form
26 September 2018
Accepted 29 September 2018
Available online 8 October 2018

Keywords:
Multiferroic
Structural transformation
Ferroelectricity

ABSTRACT

The structural, magnetic, ferroelectric and electrical properties of a series of (1-x)$BiFeO_3$-$xBa_{0.5}Sr_{0.5}MnO_3$ ($0 \le x \le 1$) solid solutions have been studied. The crystal structure of these samples changes from rhombohedral $R3c$ ($0 \le x \le 0.1$) to cubic $Pm\bar{3}m$ ($0.16 \le x \le 0.5$) and finally to hexagonal $P6_3/mmc$ ($0.7 \le x \le 1.0$) with increasing x. Two local maxima in the remnant magnetization M_r and coercive field H_c are observed in the vicinity of the two structural phase boundaries, i.e., $x = 0.16$ and 0.7. The samples with $x \le 0.1$ exhibit multiferroicity with magnetoelectric effect, while the samples with $x \ge 0.16$ possessing centrosymmetric crystal structure show semiconducting behavior. The existence of low-valence Mn^{3+} ions associated with oxygen vacancies is found to influence significantly the structure, magnetism and ferroelectricity in these samples.

1. Introduction

Multiferroic materials, showing simultaneously magnetism and ferroelectricity orders, have been widely studied in recent years due to their potential applications in data storage, sensors, and so on [1,2]. The magnetic and ferroelectric (FE) ordering parameters in multiferroics are coupled to each other, giving rise to the magnetoelectric (ME) effect [3,4]. The multiferroic $BiFeO_3$ (BFO) shows magnetism and rather large FE polarization (~90–100 μC/cm^2) at room temperature (RT) [5,6]. It also possesses high FE curie temperature (T_{CE}~1100 K) and antiferromagnetic (AFM) Néel temperature (T_N~643 K) [3]. However, the high leakage current [7], small ME effect [8], and weak ferromagnetism due to the spatially modulated cycloidal spin structure in BFO prohibit its potential device application [9]. Much efforts including element substitution [10,11] and quenching [12], etc, have been made to improve the multiferroicity and ME effect in BFO.

It is noted that $Sr_{0.5}Ba_{0.5}MnO_3$ (BSMO) was recently reported to be multiferroic with non-centrosymmetric tetragonal structure. In BSMO the FE Curie temperature is above RT (>400 K), and the saturation FE polarization can reach ~25 μC/cm^2 [13]. Both the experimental results and theoretical calculations show that the ferroelectricity of the BSMO system arises from the off-center displacement of B-site Mn^{4+} ion [13,14], which is similar to the case of the prototype FE $BaTiO_3$. Since both the ferroelectricity and magnetism originate from the same Mn^{4+} ion, the ME coupling in BSMO was suggested to be very strong. However, this system is AFM, and the Néel temperature is low ($T_N < 200$ K) [13,14]. On the other hand, it is also noted that Fe^{3+} possesses an electron configuration of d^5, while Mn^{4+} has a d^3 configuration. According to the Goodenough-Kanamori (G-K) rules [21,22], the d^5-d^3 type magnetic interaction between transition metal ions should be ferromagnetic (FM)/ferrimagnetic (FIM). Actually, FM or FIM interaction was predicted and experimentally found between $Fe^{3+}(d^5)$-$Cr^{3+}(d^3)$ in Bi_2FeCrO_6 and La_2FeCrO_6 [15,16]. Therefore, it is expected that multiferroicity with strong magnetization could be found in the solid solutions between BFO and BSMO.

In the present work, we studied in detail the structural, magnetic, and FE properties in (1-x)BFO-xBSMO ($0 \le x \le 1$) solid solutions. It is interesting that we found two structural phase boundaries around x~0.16 and 0.7, respectively, which exhibit the

* Corresponding author.
** Corresponding author.
E-mail addresses: lhyin@issp.ac.cn (L.H. Yin), whsong@issp.ac.cn (W.H. Song).

https://doi.org/10.1016/j.jallcom.2018.09.388
0925-8388/

maximum magnetization, in (1-*x*)BFO-*x*BSMO. Moreover, multiferroicity were observed in $x \leq 0.1$. The valence of Mn ions was found to play an important role in the crystal structure and multiferroicity in the (1-*x*)BFO-*x*BSMO system.

2. Experimental

Polycrystalline samples (1-*x*)BFO-*x*BSMO ($0 \leq x \leq 1$) were prepared with the sol-gel method. Stoichiometric amounts of $Bi(NO_3)_3 \cdot 5H_2O$, $Ba(NO_3)_2$, $Fe(NO_3)_3 \cdot 9H_2O$, $SrCO_3$ and $MnC_4H_6O_4 \cdot 4H_2O$ were used as the starting materials and were dissolved in nitric acid. Polyethylene glycol was added to the solution as a complexant and the mixture was stirred until a transparent precursor solution was obtained. Then, the precursor solutions were heated in an oven at 90 °C for a whole night, resulting in the formation of a gel. The gel was decomposed at 400 °C for 2 h, and the resulting porous powders were ground and pressed into 13-mm-diameter disks at a pressure of 14 MPa, and then fired at 700 °C for 2 h. The disks were reground and pressed into 13-mm-diameter disks at a pressure of 14 MPa. The final sintering temperatures for all the samples were 800 °C for 2 h ($x = 0$), 850 °C for 2 h ($x = 0.05$), 900 °C for 2 h ($x = 0.1$), 1000 °C for 2 h ($x = 0.16, 0.23, 0.3$), 1100 °C for 20 h ($x = 0.5, 0.7, 0.9, 1$). Part of the as-prepared samples were further annealed in a flowing oxygen atmosphere (the flow rate is 50 sccm) at 870 °C for 5 h. The density of the sintered samples ($0.05 \leq x \leq 1$), which was determined by using the Archimedes' principle, are about 8.01, 7.52, 7.02, 6.16, 6.44, 5.71, 6.58, 3.81 and 3.33 g/cm^3, respectively. The RT X-ray diffraction (XRD) measurement was carried out with a Philips X'pert PRO x-ray diffractometer using Cu K_α radiation. The Raman scattering measurements were performed using a Horiba Jobin Yvon T64000 Micro-Raman instrument with a Kr^+-Ar^+ mixed gas laser ($\lambda = 532$ nm) as an excitation source in a backscattering geometry, and the laser power was kept at ~2.5 mW to avoid local heating effect. The FE polarization, and leakage current were measured by using a FE test system (Precision LC, Radiant Technologies). Dielectric measurements were performed with a commercial LCR meter (TH2828S) at different frequencies (1–1000 kHz) ($300 \leq T \leq 1000$ K). For the FE and dielectric measurements, the samples were cut into slices of about 0.2 mm in thickness using a low-speed diamond cutting machine, and silver epoxy electrical contacts were applied onto both sides of the slices. The surface morphology analyses of the samples were carried out by a field-emission scanning electron microscopy (FE-SEM, SU 8020, HITACHI). X-ray photoelectron spectroscopy (XPS) measurement was carried out in a Thermo ESCALAB 250Xi using monochromatic Al K_α source ($P = 150$ W, $h\nu = 1486.6$ eV). The magnetic measurements were performed using the Quantum Design (QD) superconducting quantum interface device (SQUID) ($2 \leq T \leq 380$ K, $0 \leq H \leq 4.5$ T). The Seebeck coefficient *S* was measured by a four-probe method on QD physical property measurement system (PPMS-9T).

3. Results and discussions

3.1. Structure

The RT XRD patterns of (1-*x*)BFO-*x*BSMO ($0 \leq x \leq 1$) samples are shown in Fig. 1. All the samples are single phase except for $x = 0$ and $x = 1$, which is due to the unstable structure of the two end members. In fact, it has been challenging to obtain kinetically unstable single-phase BFO due to the kinetic formation of other Bi and Fe based impurity phases as well as the narrow sintering temperature range of BFO [17,18]. While for BSMO, it is chemically unstable due to the metastable perovskite structure with nominal 4 + Mn oxidation state [19].

As clearly seen from Fig. 1(b) and (c), the two double peaks around the diffraction angle 2θ of 32° and 52°, respectively, gradually merged into two single peaks, respectively, with *x* increasing to 0.16, which indicates a structural phase transition. With further increasing *x* to about 0.7, the single peak around $2\theta = 32°$ split into two peaks and the peak around $2\theta = 52°$ gradually disappeared, implying another structural transition.

The Rietveld analysis of the powder XRD patterns suggests the crystal structures of rhombohedral *R*3*c*, cubic $Pm\bar{3}m$ and hexagonal $P6_3/mmc$ for the samples with $0 \leq x \leq 0.1$, $0.16 \leq x \leq 0.5$ and $0.7 \leq x \leq 1.0$, respectively. The experimental and calculated powder XRD patterns for the representative samples $x = 0.1$, 0.3 and 0.9 are plotted in Fig. 2. It is found that the samples with $x = 0.16$ and 0.7,

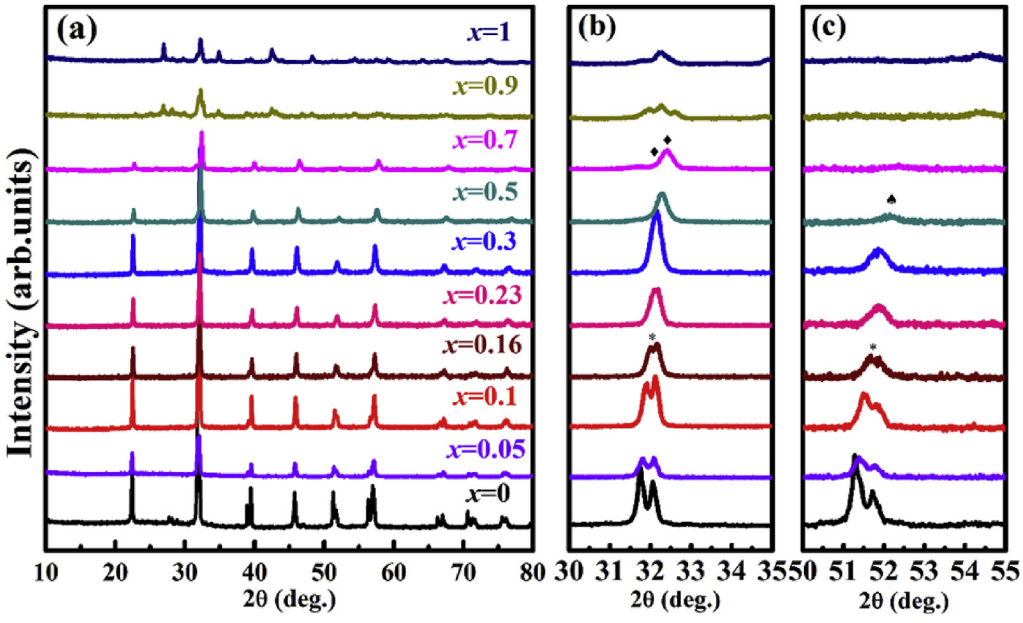

Fig. 1. The RT XRD patterns for (1-*x*)BFO-*x*BSMO ($0 \leq x \leq 1$) samples; *, ◆, and ♠ indicate the structural phase transition.